



Room Temperature Synthesis of Alloy Nanoparticles

Summer R. Ferreira, Tina M. Nenoff, Zhenyuan Zhang,
Jianyu Huang, Kevin Leung, Donald T. Berry

Sandia National Laboratories
Albuquerque, NM 87185 USA

ACS
Division of Inorganic Chemistry:
Nanoscience
Anaheim CA
March 30, 2011

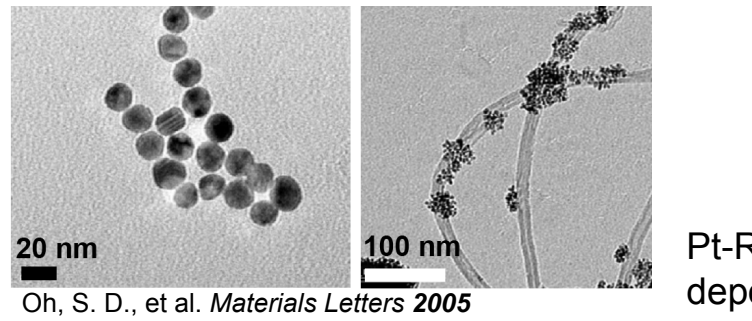


Radiolysis to Form Novel Alloys Meta-Stable Phase Spaces

Radiolysis by γ -radiation is used to access new alloys

By varying the dose rate, we vary the structure of nanoparticle growth in solution over a wide composition range in alloys

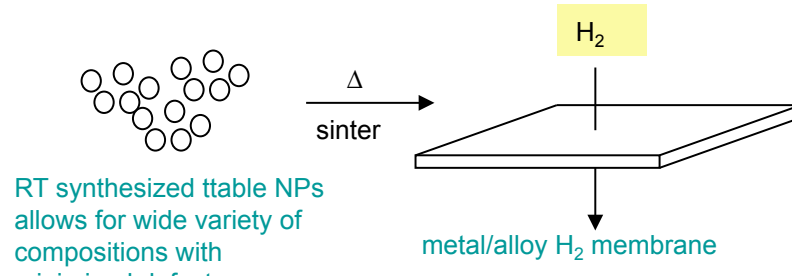
Reactions occur at room temperature allowing for growth on various substrates



Pt-Ru NP grown and deposition on SWCNT

Sintered materials for: H_2 membranes, gas turbine microengines, lightweight aircraft, etc.

- **State of the Art: Pd and Pd-alloys for durable H_2 dissociative membranes operate at high temperatures and are CO and sulfur tolerant**

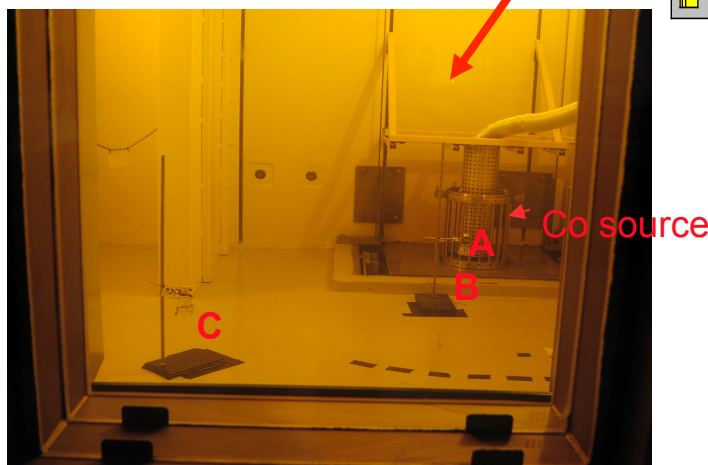
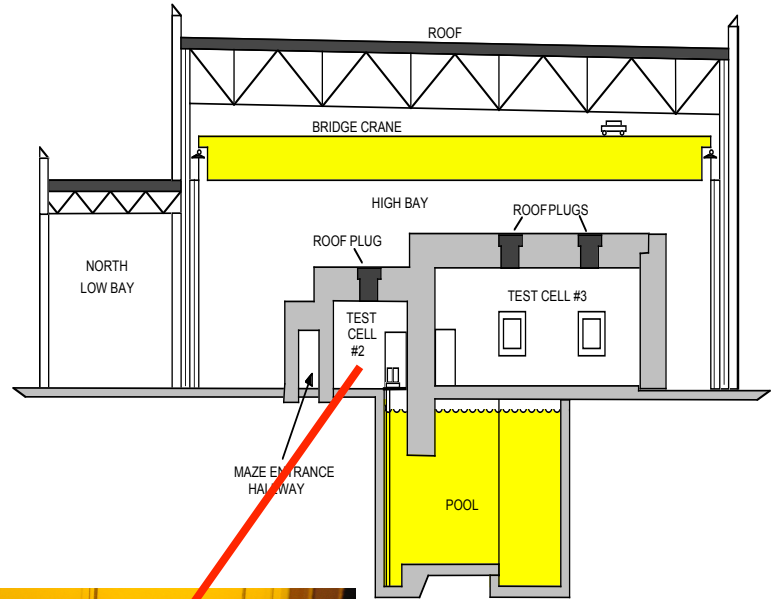


RT synthesized ttable NPs allows for wide variety of compositions with minimized defects



Room Temp Radiolysis at Sandia (SNL) GIF Facility

Sandia Gamma Irradiation Facility (GIF) is a
 ^{60}Co source : 1.345×10^5 Ci, $\approx 300\text{K}$ rad/hr.

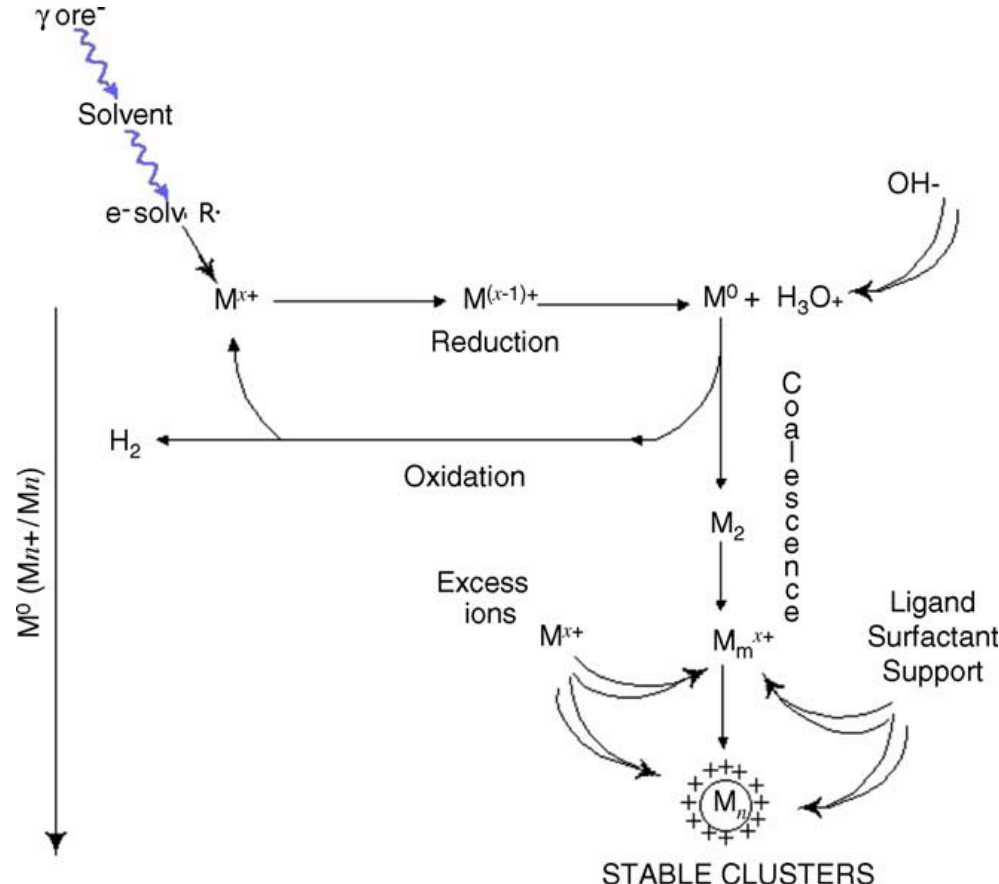




Radiolysis for Nanoparticle Formation

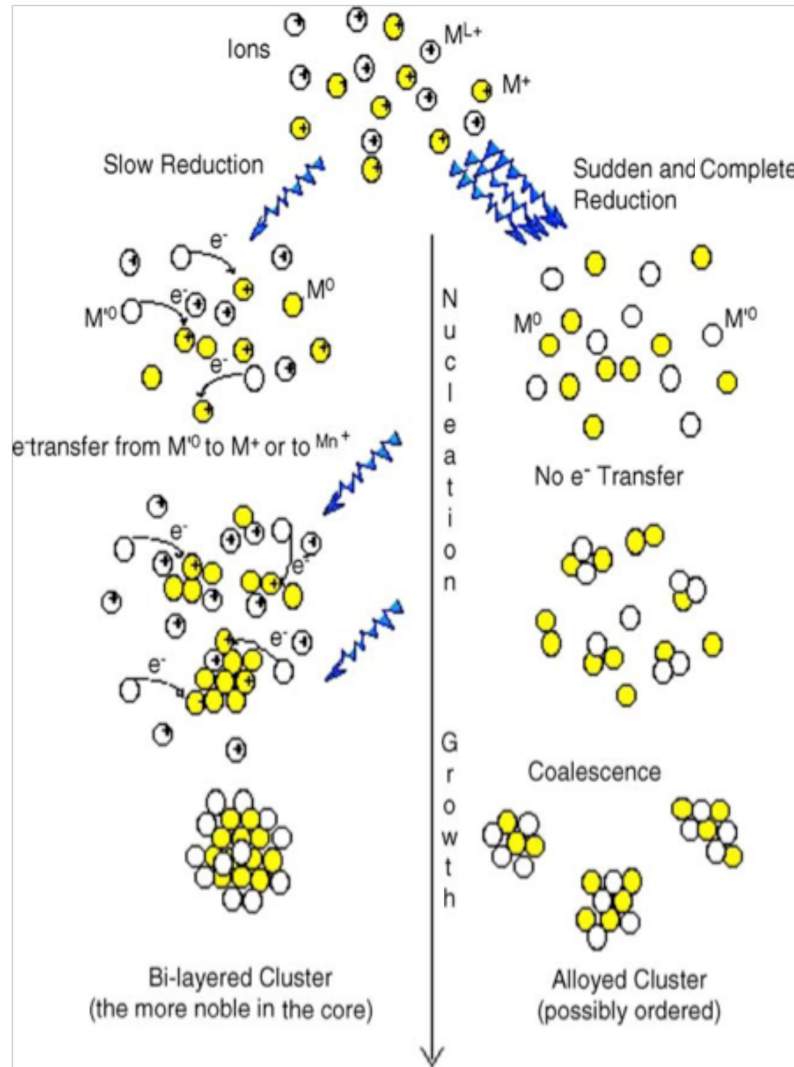
Metal ion reduction by ionizing radiation:

Dose rate dictates $[e^-]$ in reaction solution thereby affecting the chemistry of the NP formation





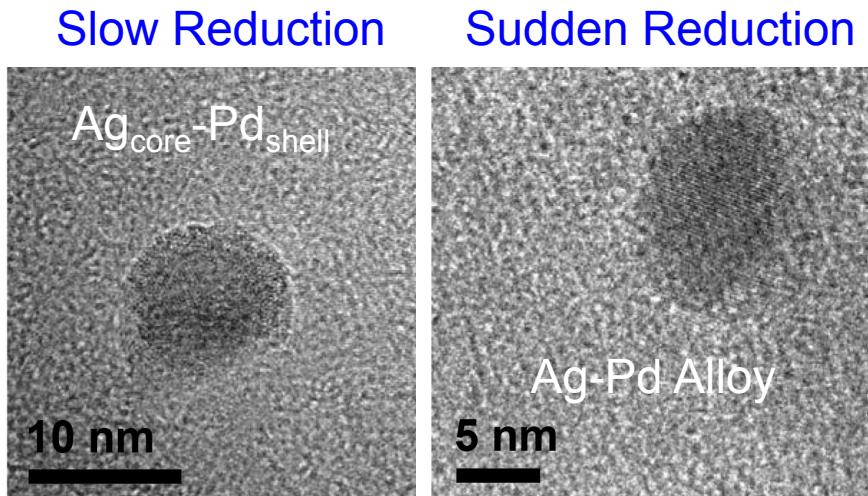
Methodology to Access Ni-based Alloy Phase Spaces



Belloni, *Catalysis Today*, 2006, 113, 141

Alloys: Possibility to access different phase space than with traditional melting

Using **high radiation dose** and **High dose rate**, we pursue nanoparticle alloy formation



Redjala, T. et al. *Oil Gas Sci. Technol.* 2006

$AgNO_3$, $HAuCl_4$, $Pd(NO_3)_2$ and poly (vinyl alcohol) (PVA, 99% hydrolysed, MW = 86000); Dose rate of 1.75 Gy.s⁻¹

srferre@sandia.gov



Nanoparticle (NP) Synthesis & Analysis

Experimental NP Synthesis:

Into 25ml solutions in 100ml vials add dilute metal salt solutions, alcohol (MeOH), organic polymer (PVA) and DI H₂O.

Purged solution with N₂, sealed and stored in dark.

Exposed solutions to γ -irradiation.

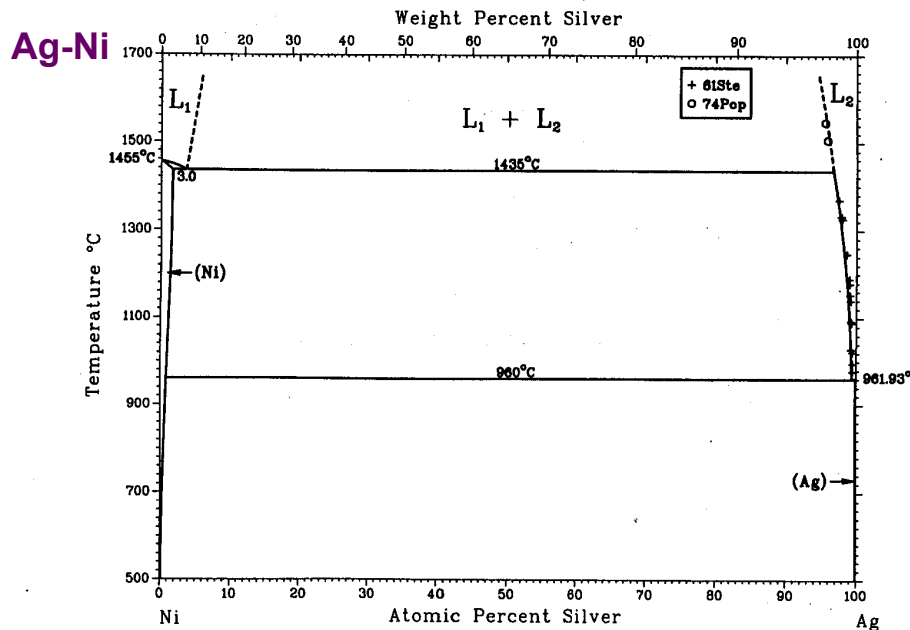
NP Analysis:

- (1) UV-vis: Varian Cary 300 Scan UV-visible Spectrophotometer
- (2) Transmission Electron Microscopy (TEM): JEOL 1200EX (120 kV) bright-field
- (3) High Resolution TEM and scanning TEM: FEI Tecnai G(2) F30 S-Twin (300 kV) TEM at Sandia's Center for Integrated Nanotechnologies (SNL CINT)
 - 0.14 nm resolution in high-angle annular dark-field (HAADF) mode
 - equipped with energy-dispersive X-ray (EDX) & electron energy-loss spectrometer (EELS)



Ag-Ni Alloy Particle Formation – Kinetically Driven Access to New Phases

Thermodynamic Phase Diagram



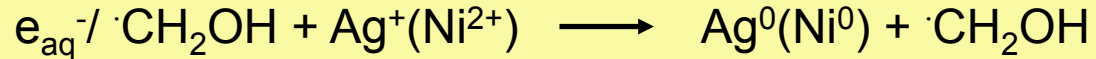
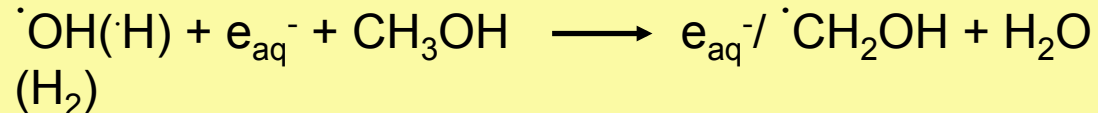
T. B. Massalski, *ASM International*, 2nd Ed., 1990

High Dose
Radiolysis: RT
Kinetic Phase
Growth

Dose Rate ≈
300 rad/sec

srferre@sandia.gov

Particle Formation via radiolysis (γ -irradiation)



Particle Growth

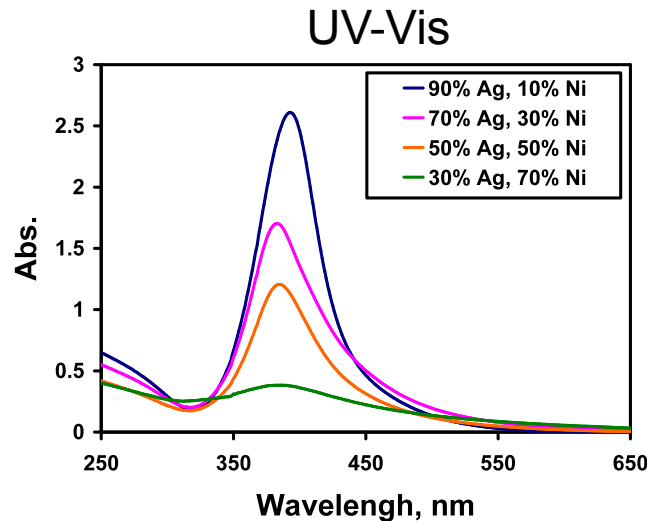




Ag-Ni Alloy NPs – Characterization

Different stoichiometries of Ag^+ and Ni^{2+} used to prepare Ag-Ni alloy NPs

	Ag	$\text{Ag}_{0.9}\text{-Ni}_{0.1}$	$\text{Ag}_{0.7}\text{-Ni}_{0.3}$	$\text{Ag}_{0.5}\text{-Ni}_{0.5}$	$\text{Ag}_{0.3}\text{-Ni}_{0.7}$	Ni
$[\text{Ag}^+], \times 10^{-4} \text{ M}$	2	1.8	1.4	1	0.6	0
$[\text{Ni}^{2+}], \times 10^{-4} \text{ M}$	0	0.2	0.6	1	1.4	2
$[\text{Ag}^+] + [\text{Ni}^{2+}], \times 10^{-4} \text{ M}$	2	2	2	2	2	2
$[\text{Ag}^+]:[\text{Ni}^{2+}]$	pure Ag NPs	9:1	7:3	5:5	3:7	pure Ni NPs



AgClO₄ and NiSO₄ are used to synthesize Ag-Ni particles by radiolysis. UV-vis spectroscopy supports varied stoichiometries in NPs.

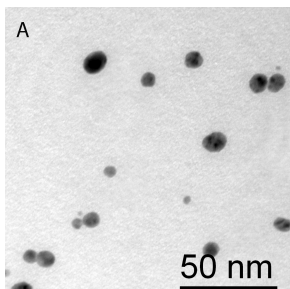
Ag plasmon band dampens from $\text{Ag}_{0.9}\text{-Ni}_{0.1}$ to $\text{Ag}_{0.3}\text{-Ni}_{0.7}$

srferre@sandia.gov

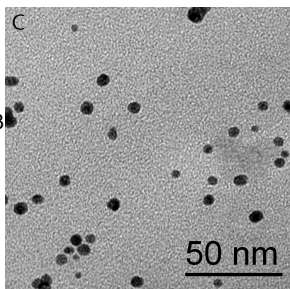


Ag-Ni Alloy NPs – TEM Images

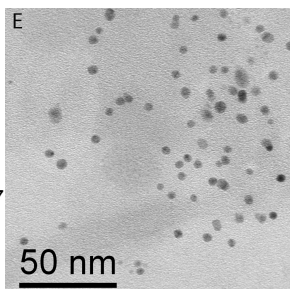
pure Ag
8.5 nm



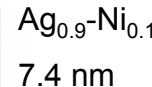
$\text{Ag}_{0.7}\text{-Ni}_{0.3}$
5.7 nm



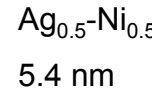
$\text{Ag}_{0.3}\text{-Ni}_{0.7}$
4.0 nm



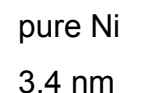
$\text{Ag}_{0.9}\text{-Ni}_{0.1}$
7.4 nm



$\text{Ag}_{0.5}\text{-Ni}_{0.5}$
5.4 nm



pure Ni
3.4 nm

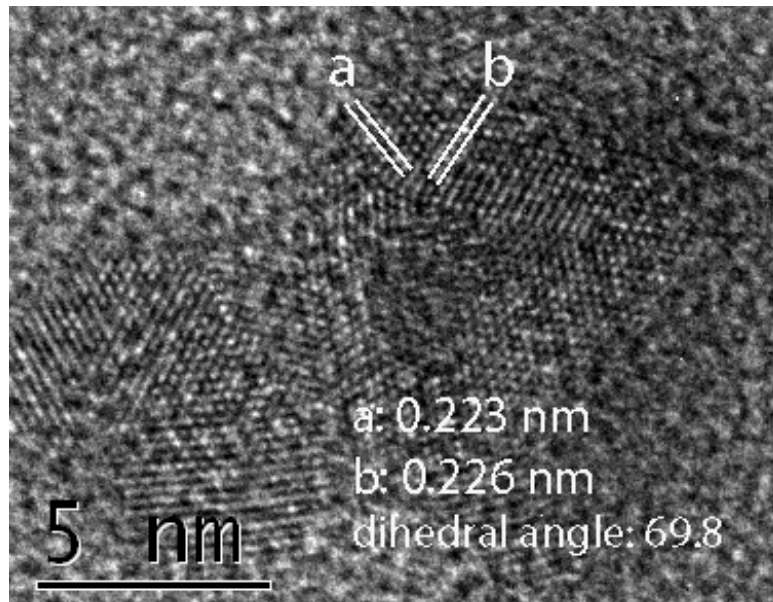


Particle size in diameter and size distribution of Ag, Ag-Ni, and Ni NPs

	Ag	$\text{Ag}_{0.9}\text{-Ni}_{0.1}$	$\text{Ag}_{0.7}\text{-Ni}_{0.3}$	$\text{Ag}_{0.5}\text{-Ni}_{0.5}$	$\text{Ag}_{0.3}\text{-Ni}_{0.7}$	Ni
size in diameter, nm	8.5	7.4	5.7	5.4	4.0	3.4
size distribution	24%	24%	20%	15%	18%	19%

The size of Ag-Ni NPs is decreased with higher Ni ratio

srferre@sandia.gov

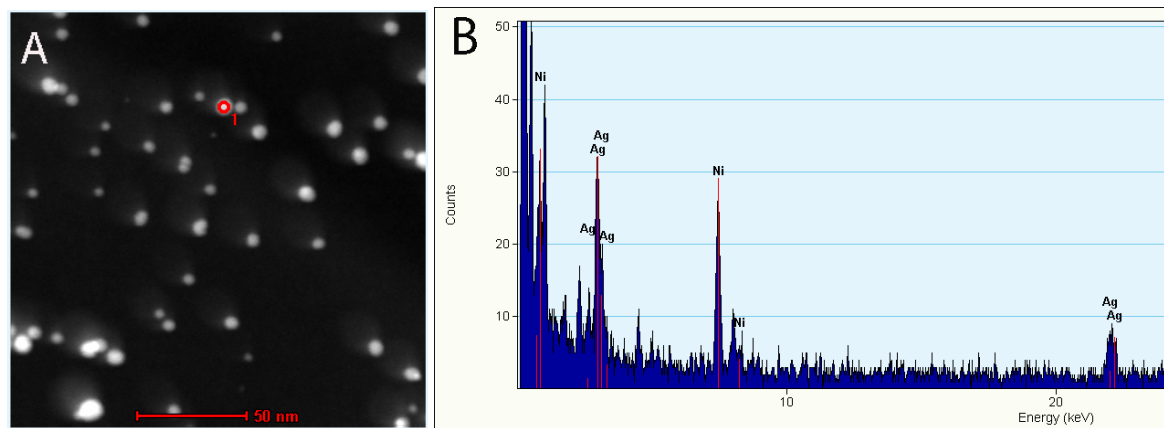


Ni: 0.203 nm, Ag: 0.236 nm Ag-Ni
Lattice spacing of 50% Ag and 50% Ni may be present. Theory: 0.220 nm



Ag-Ni Alloy NPs – HAADF Images

HAADF-STEM and single particle EDX images



$\text{Ag}_{0.5}\text{-Ni}_{0.5}$ NPs

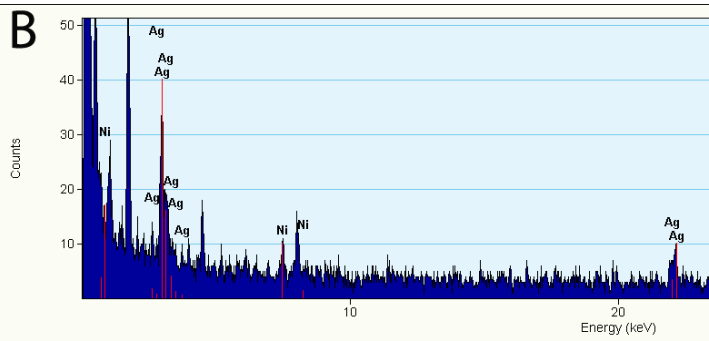
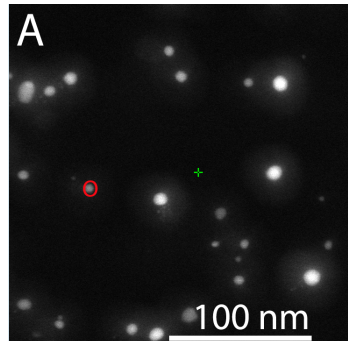
The size of Ag and Ni peaks from single particle EDX are comparable in intensity

JPCC, 2009, 113, 1155; US Patent Tech Advance, 2008: SD10767

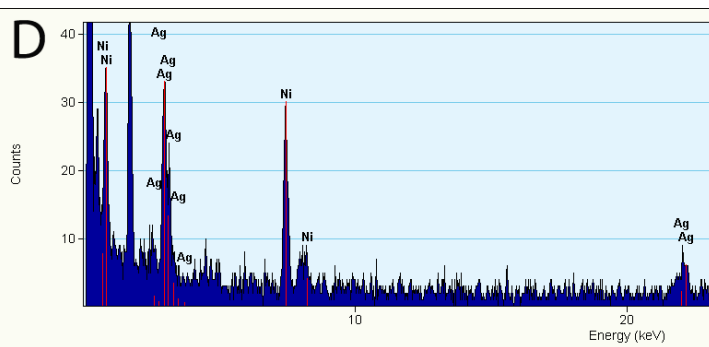
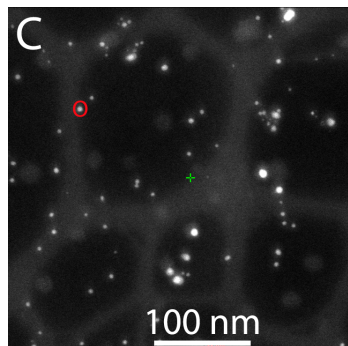
srferre@sandia.gov



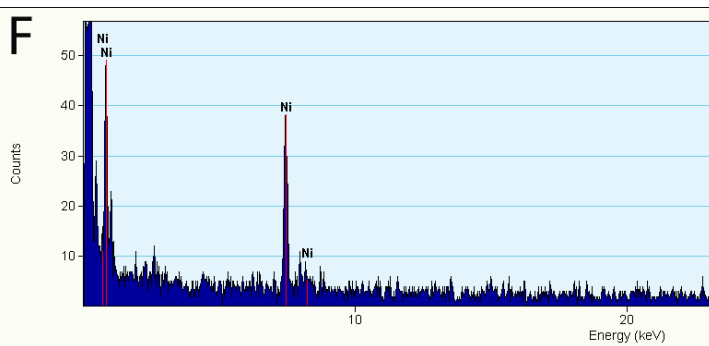
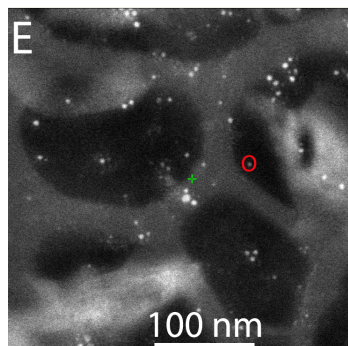
Ag-Ni Alloy NPs – HAADF Images



$\text{Ag}_{0.7}\text{-Ni}_{0.3}$ NPs



$\text{Ag}_{0.3}\text{-Ni}_{0.7}$ NPs



pure Ni NPs

srferre@sandia.gov

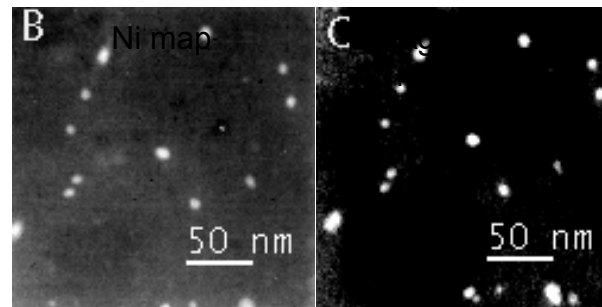
The size of Ag and Ni peaks qualitatively correspond to initial ion ratios



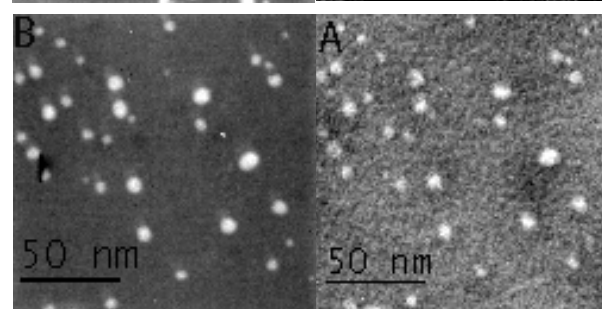
Ag-Ni Alloy NPs – EFTEM Mapping

EFTEM maps

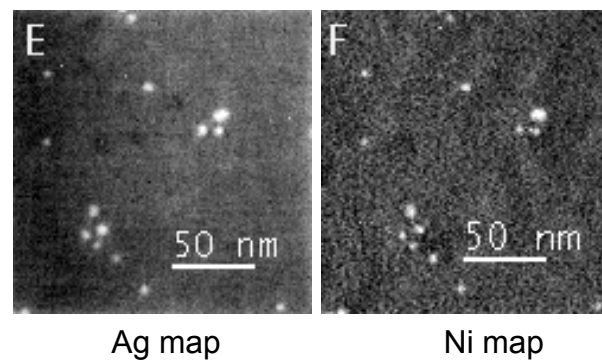
$\text{Ag}_{0.7}\text{-Ni}_{0.3}$ NPs



$\text{Ag}_{0.5}\text{-Ni}_{0.5}$ NPs



$\text{Ag}_{0.3}\text{-Ni}_{0.7}$ NPs



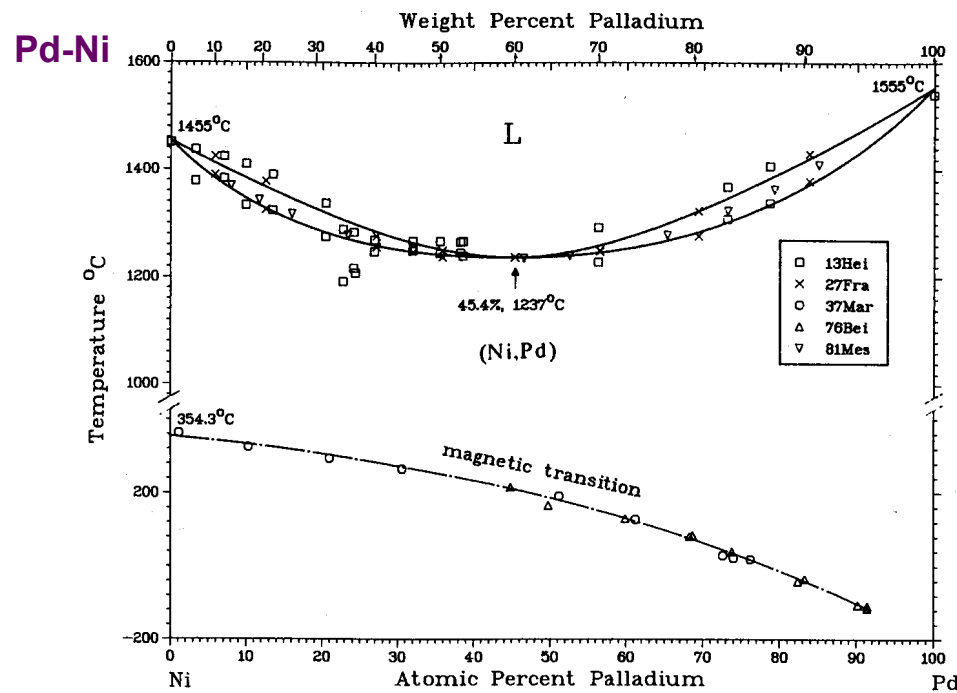
Elemental mapping shows Ag and Ni concentrated uniformly in NPs

srferre@sandia.gov



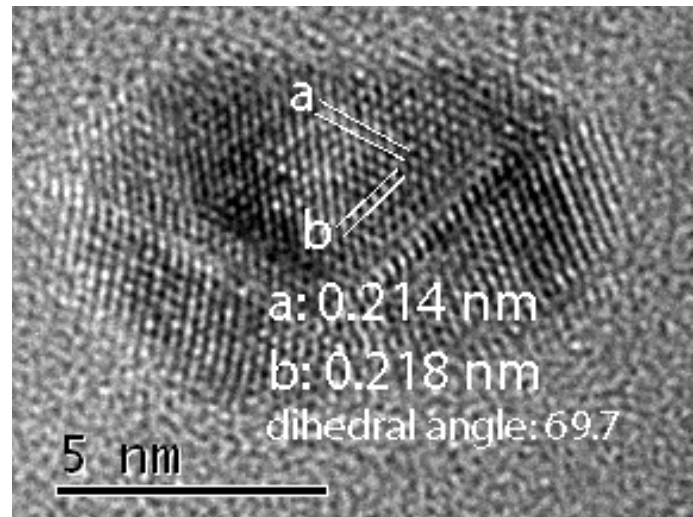
Pd-Ni Alloy Nanoparticles

Pd-Ni NPs: 50% Ni, 50% Pd



T. B. Massalski, *ASM International*, 2nd Ed., 1990

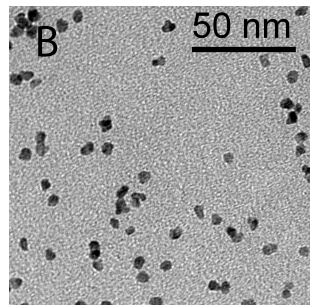
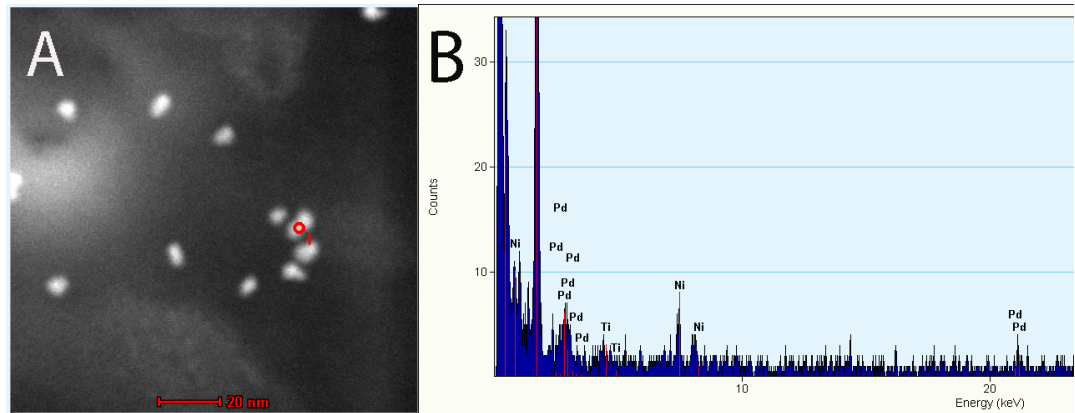
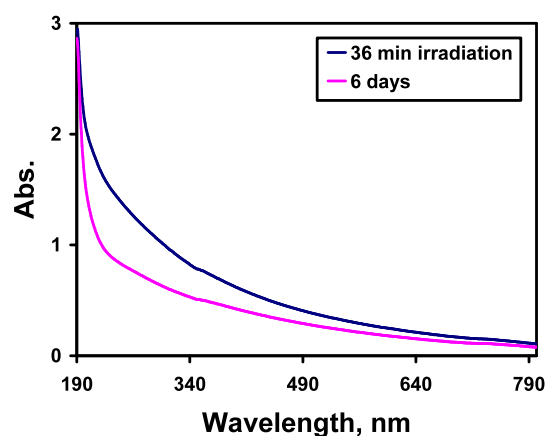
HRTEM (CINT): (twinned crystal)
Ni (111) = 0.203 nm, Pd (111) = 0.225 nm
Pd-Ni alloy based on 50% Ni = 0.214 nm



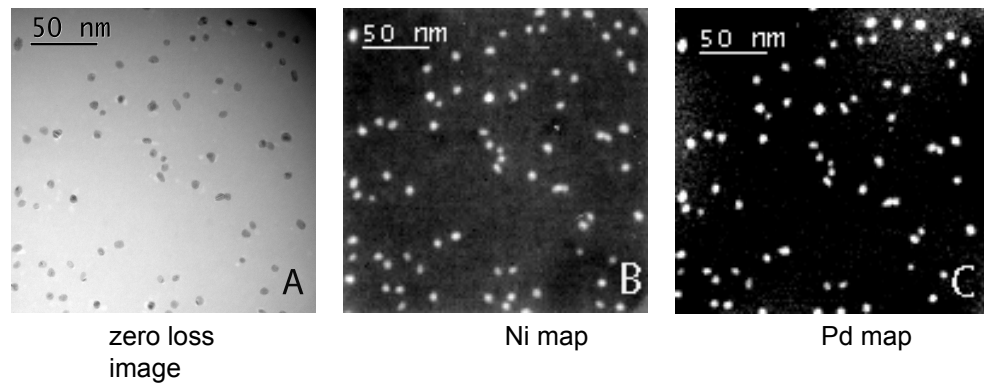


Characterization of Pd-Ni Alloy NPs

$\text{Pd}(\text{NH}_3)_4\text{Cl}_2$ and NiSO_4 are used to synthesize $\text{Pd}_{0.5}\text{-Ni}_{0.5}$ particles by radiolysis (high dose rate, 300 rad/s)



HAADF-STEM and single particle EDX images



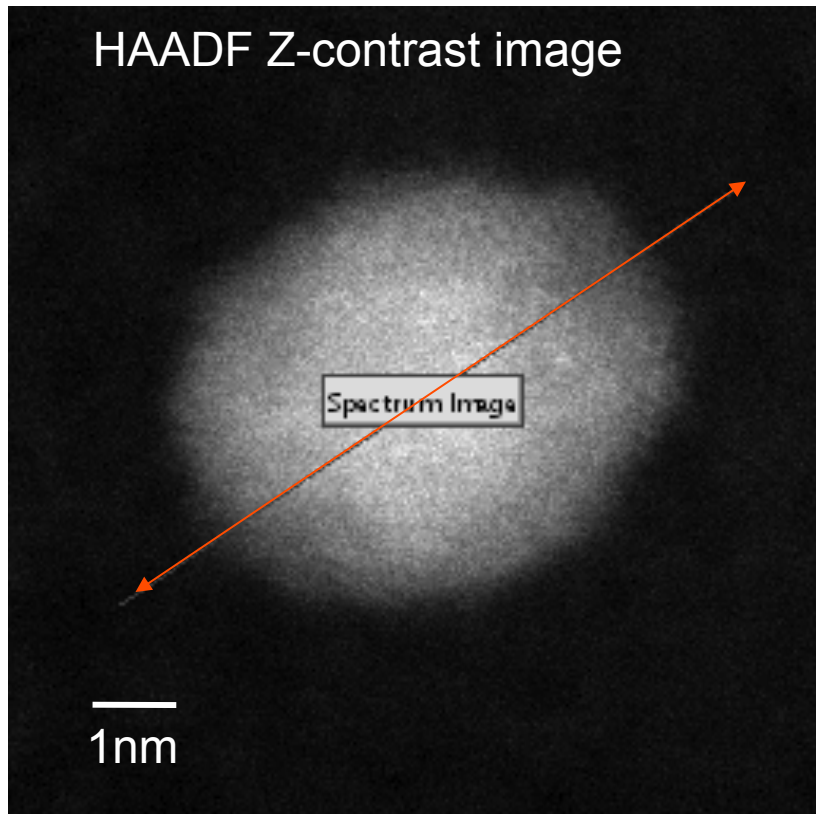
- STEM & EDX: Single particle data indicates homogenous composition of Pd & Ni

srferre@sandia.gov

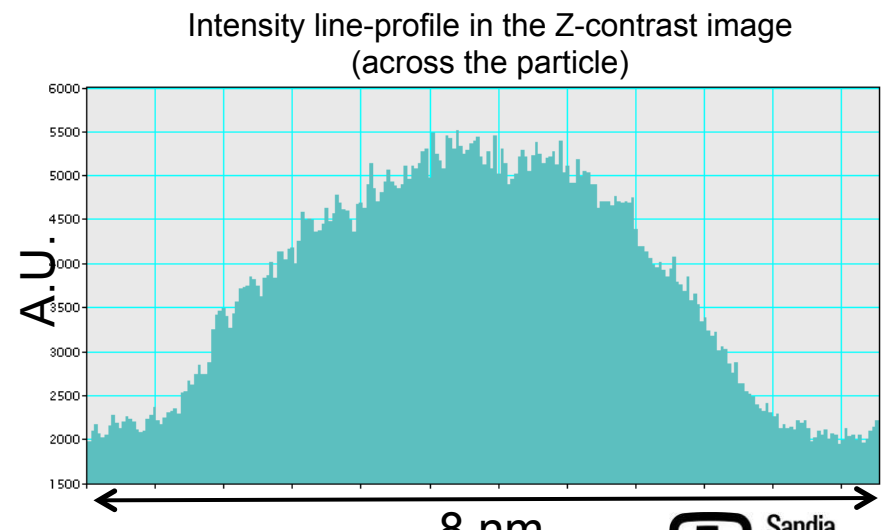
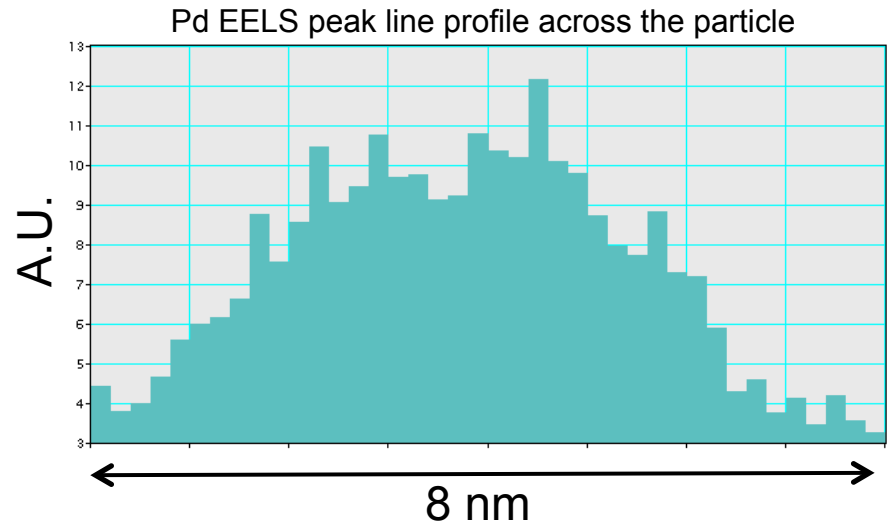
EFTEM maps



Atomic resolution compositional analysis by EELS



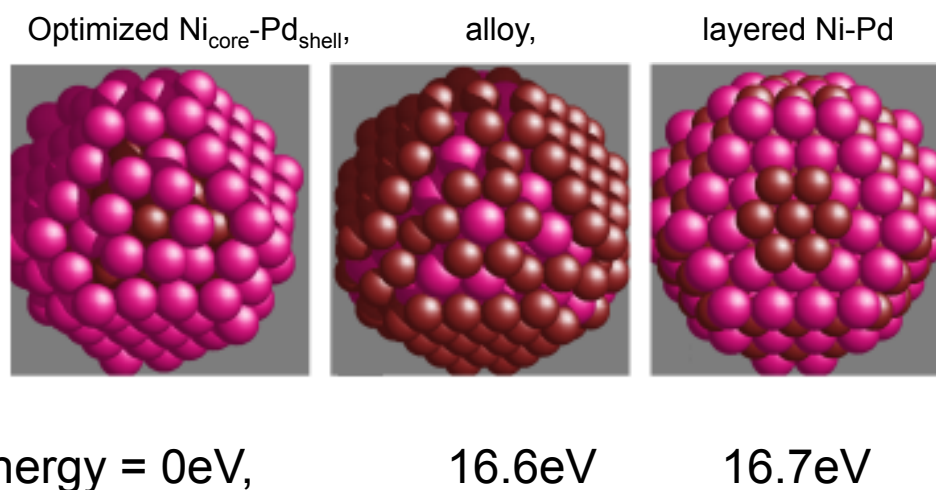
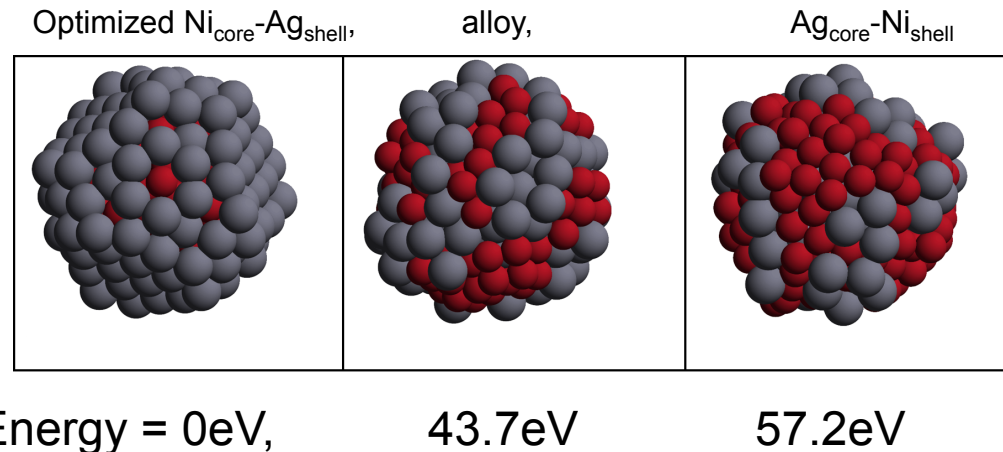
The Z contrast profile and the Pd EELS peak profile have a very similar shape, **indicating the uniform distribution of Pd atoms in the particle**





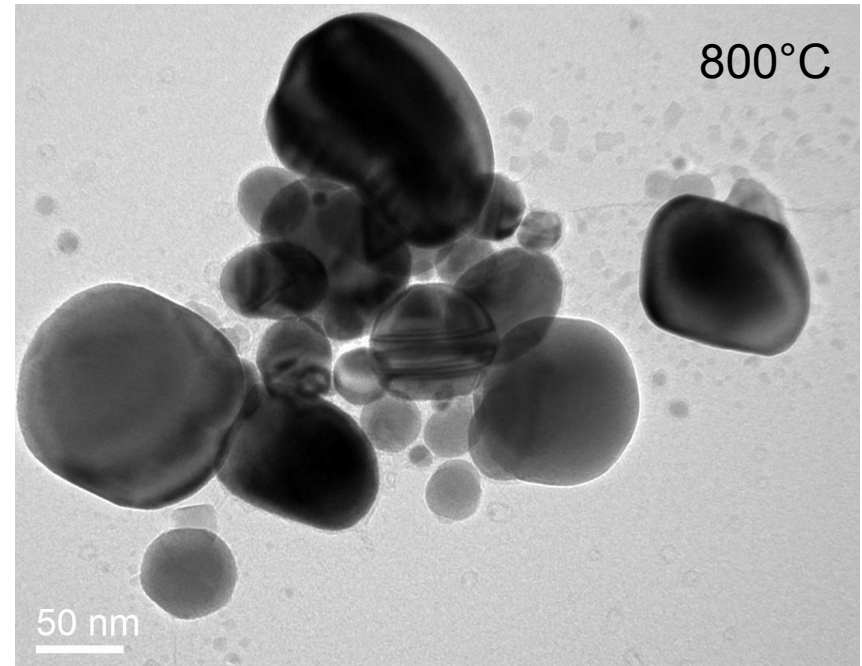
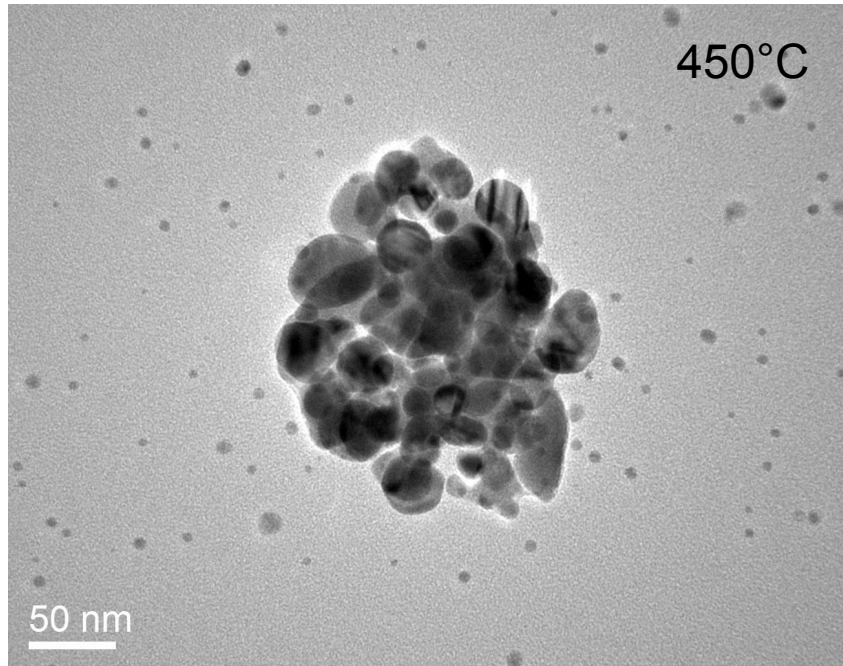
Kinetically Driven Alloy Phase Formations – Confirmed with 1st Principles Modeling

DFT Modeling using the VASP Code; FCC simulation using 240 atoms/NP





Sintering Ag-Ni NPs: 25°C – 800°C on heated TEM stage



50/50 AgNi, small scale ripening from RT - 450°C in first 25 min

Rapid large scale sintering, possibly *via* Oswald Ripening processes, occurs in \approx 15 min. between 450 – 800°C

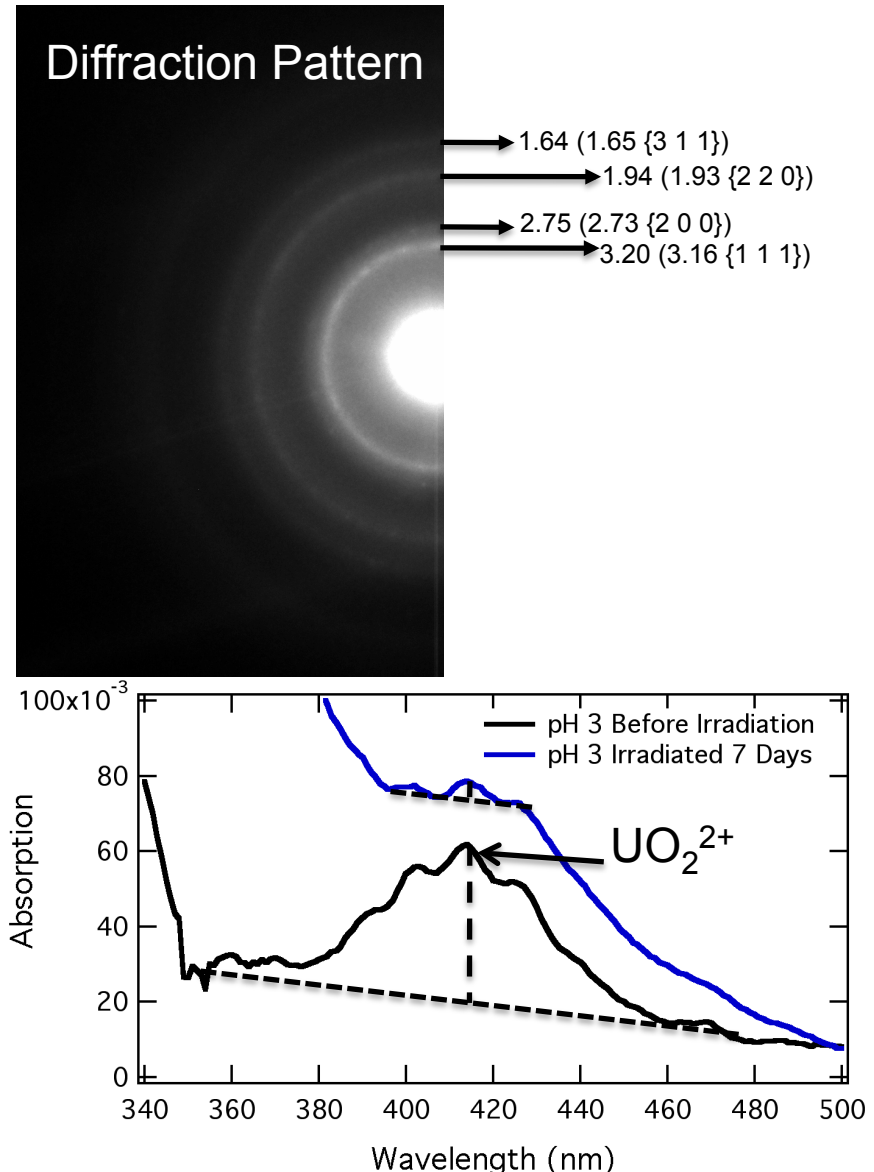
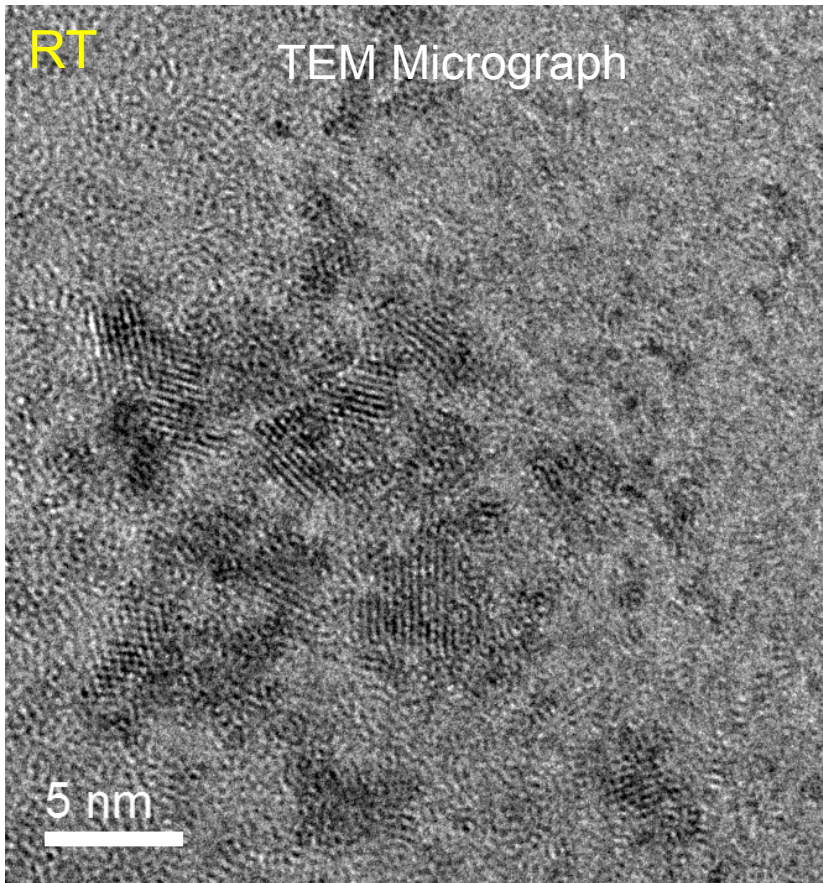
Melting Points: Ag 962 °C
Ni 1453 °C

srferre@sandia.gov

 Sandia
National
Laboratories



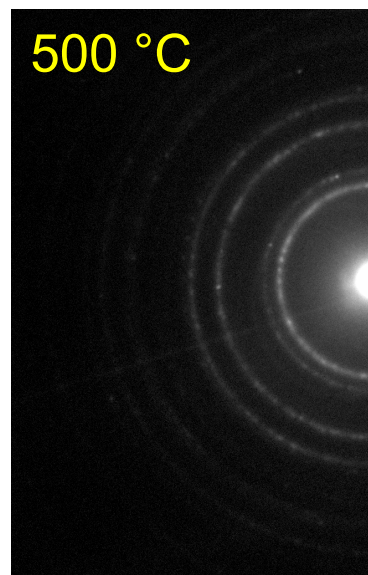
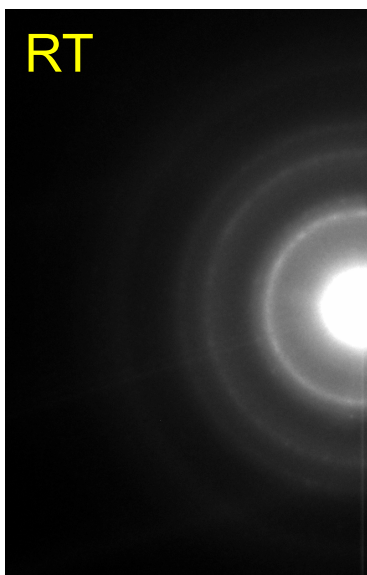
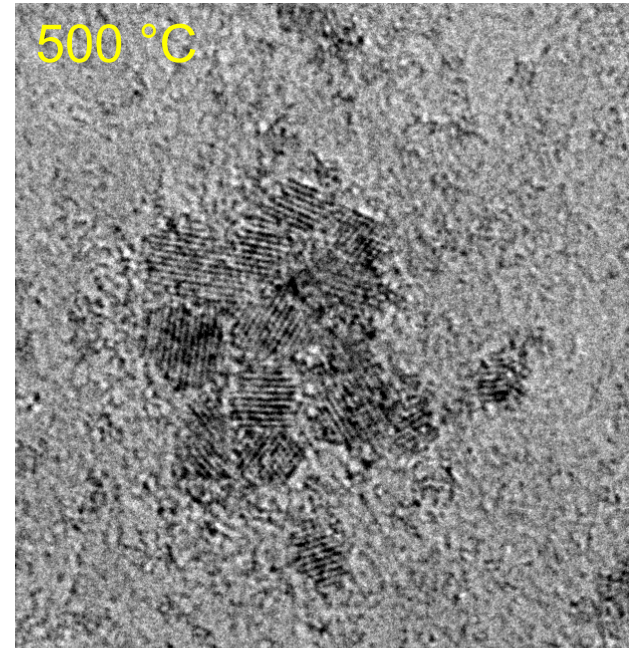
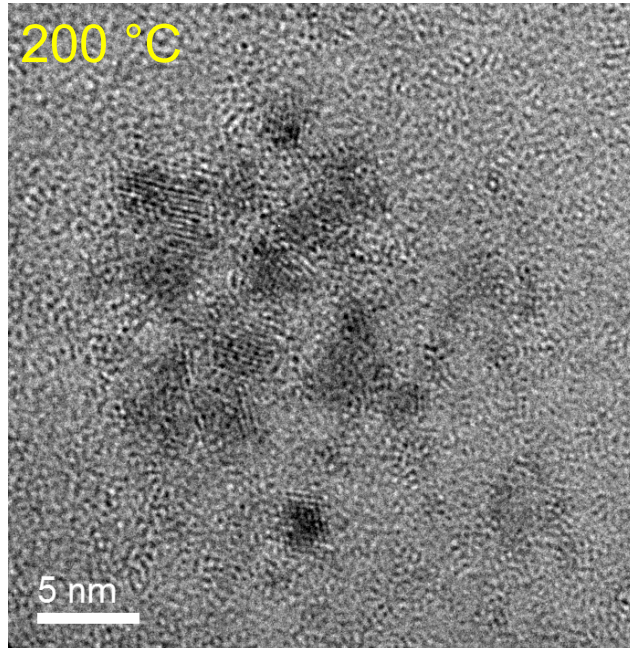
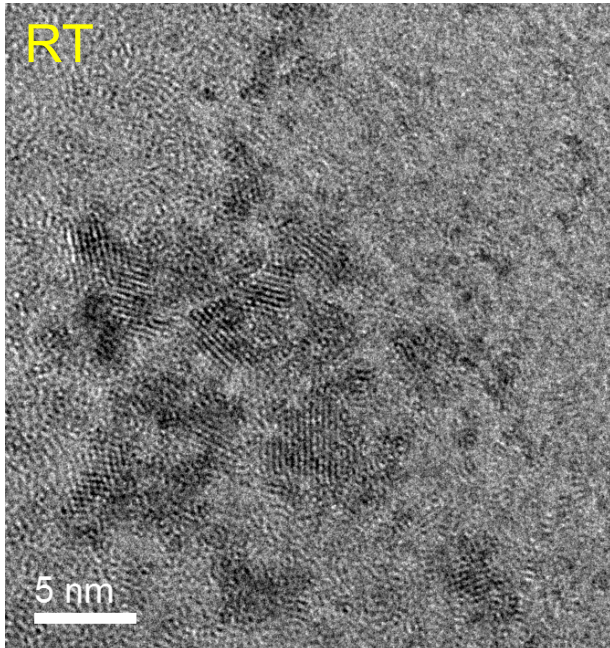
Characterization of U containing NPs



UO_2 NP formation confirmed
by UV-vis, bright-field TEM
and diffraction



UO₂ NP Sintering at 500 °C



Low T NP
sintering
achieved at
500 °C; ~1000
°C lower than
reported

9:30 am Lanthanide and
Actinide Chemistry



Conclusions

- **Ag and Ni are immiscible. Ag-Ni NPs are considered a core-shell structure from both experiments and simulations.**
- **Low dose rate** intermetallic electron transfer causes core-shell formation
- **High dose rate, alloyed Ag-Ni & Pd-Ni NPs are formed.** Rate overrides electrochemical or thermodynamic process, and competes with possible intermetallic electron transfer.

High dose rate reduces ions very fast, so high dose rates favor alloy formation

- **DFT modeling supports alloy formation at high dose rate**
- **Sintering of alloy NPs from $\approx 5\text{nm}$ NPs to large / mesoscale bulk formation**



Acknowledgements

Team Members

Synthesis: Zhenyuan (Mark) Zhang, Donald T. Berry

TEM: Jianyu Huang, Paula Provencio

NP Sintering/ Heated Stage TEM: David Robinson, Benjamin Jacobs

Modeling: Roland Stumpf, Kevin Leung

Funding

This work was supported in part by the Laboratory Directed Research and Development (LDRD) program of Sandia National Laboratories.

Sandia National Laboratories is a multiprogram laboratory operated by Sandia Corporation, a Lockheed Martin Company, for the United States Department of Energy's National Nuclear Security Administration under contract DE-AC04-94AL85000.



srferre@sandia.gov

